

Arsenic disulfide-induced apoptosis and its potential mechanism in two- and three-dimensionally cultured human breast cancer MCF-7 cells

YUXUE ZHAO^{1,2}, KENJI ONDA¹, BO YUAN³, SACHIKO TANAKA¹, ANNA KIYOMI⁴, KENTARO SUGIYAMA¹,
MUNETOSHI SUGIURA⁴, NORIO TAKAGI³ and TOSHIHIKO HIRANO¹

¹Department of Clinical Pharmacology, School of Pharmacy, Tokyo University of Pharmacy and Life Sciences, Hachioji, Tokyo 192-0392, Japan; ²Institute of Acupuncture and Moxibustion, China Academy of Chinese Medical Sciences, Beijing 100700, P.R. China; Departments of ³Applied Biochemistry and ⁴Drug Safety and Risk Management, School of Pharmacy, Tokyo University of Pharmacy and Life Sciences, Hachioji, Tokyo 192-0392, Japan

Received September 13, 2017; Accepted February 27, 2018

DOI: 10.3892/ijo.2018.4357

Abstract. In China, arsenic disulfide (As_2S_2) has been used for the treatment of hematological malignancies. The present study aimed to evaluate the effects of As_2S_2 on the human breast cancer MCF-7 cell line cultured in both two-dimensional (2D) monolayers and three-dimensional (3D) spheroids to explore its therapeutic potential in breast cancer treatment. Cellular viability and the induction of apoptosis were examined with a cell counting kit-8 (CCK-8) assay and flow cytometric analysis, respectively. Alterations in the expression levels of apoptosis-associated proteins, including Bcl-2-associated X protein (Bax), B-cell lymphoma 2 (Bcl-2), p53, and caspase-7, as well as the cell survival-associated proteins, phosphatidylinositol 3-kinase (PI3K), Akt, and mammalian target of rapamycin (mTOR), were assessed by western blotting. Although a dose-dependent reduction in cell viability, which occurred in association with the induction of apoptosis triggered by the addition of 2-24 μM As_2S_2 , was observed in both 2D- and 3D-culture systems, 3D spheroids were less sensitive to the cytotoxic effect of As_2S_2 compared with the 2D cultured

cells. A significant increase in the expression levels of Bax, p53, and caspase-7 was observed in treated 2D-cultured cells, whereas a similar increase in the expression levels of Bax was only confirmed in treated 3D spheroids, although there was a trend towards the increased expression of p53 and caspase-7 in the 3D spheroids. These results suggested that these molecules are closely associated with As_2S_2 -mediated cytotoxicity in the two culture systems, and further suggested that the difference in the sensitivity to As_2S_2 between 2D monolayers and 3D spheroids may be attributed to the differential alterations in the expression levels of proteins associated with cell mortality. Significant downregulation of the expression levels of Bcl-2, PI3K, Akt and mTOR was observed in the two culture systems. Taken together, the results of the present study demonstrated that As_2S_2 inhibits cell viability and induces apoptosis in both 2D- and 3D- cultured MCF-7 cells, which may be associated with activation of the pro-apoptotic pathway and the inhibition of pro-survival signaling. These results have provided novel insights into clinical applications of As_2S_2 in the treatment of patients with breast cancer.

Correspondence to: Professor Toshihiko Hirano, Department of Clinical Pharmacology, School of Pharmacy, Tokyo University of Pharmacy and Life Sciences, 1432-1 Horinouchi, Hachioji, Tokyo 192-0392, Japan
E-mail: hiranot@toyaku.ac.jp

Abbreviations: As_2S_2 , arsenic disulfide; 2D, two-dimensional; 3D, three-dimensional; ATO, arsenic trioxide; APL, acute promyelocytic leukemia; Bcl-2, B-cell lymphoma 2; Bax, Bcl-2-associated X protein; PI3K, phosphatidylinositol 3-kinase; mTOR, mammalian target of rapamycin; MCS, multicellular spheroid; TGP, thermo-reversible gelatin polymer; OD, optical density

Key words: arsenic disulfide, MCF-7, two-dimensional monolayer, three-dimensional spheroid, cell viability, apoptosis

Introduction

Breast cancer is one of the most common female malignancies, as well as one of the leading causes of cancer-associated morbidity and mortality in women (1,2). The standard and classical treatments for breast cancer, including surgical resection, radiotherapy and chemotherapy, are far from satisfactory due to limited efficacy and high rates of recurrence (3). Thus, the development of new therapeutic strategies is urgently needed for the treatment of breast cancer. Arsenic compounds, such as arsenic trioxide (ATO), which has been used in standard treatment strategies for acute promyelocytic leukemia (APL) (4,5), and sodium arsenite, have been reported to show cytotoxic effects against breast cancer cell lines (6-9). However, such arsenic compounds are commonly regarded as toxic compounds with adverse effects, including visceral organ damage, serious acute toxicity, and potential carcinogenicity, which consequently limit their clinical applications (10-12).

Arsenic disulfide (As₂S₂), as the predominant active ingredient of realgar, also known as 'Xiong-Huang' in traditional Chinese medicine, is considered to be a candidate for the treatment of several types of malignancies; it exhibits relatively low toxicity, and has the advantage of being orally administered (10,13-15). A series of basic and clinical studies have reported the antitumor effects of As₂S₂ in different types of malignancies, particularly hematopoietic tumors such as APL (13,16-19). Recently, there is increasing evidence to support that As₂S₂ has the ability to induce apoptosis and inhibit the growth of hematopoietic and solid tumor cell lines, such as human lymphoma cell lines (20), cervical cancer cell lines (21), human hepatocellular carcinoma cells (22), and human osteosarcoma cell lines (23). However, although the cytotoxic effect of realgar nanoparticles has been demonstrated (24), the effects of As₂S₂ on breast cancer cells, and the underlying mechanisms, have yet to be fully investigated.

In recent decades, studies on the development of three-dimensional (3D) cell culture systems to generate multicellular tumor spheroids have attracted much attention. The findings of such studies suggest that the natural manner in which solid tumor cells grow *in vivo* is in 3D, indicating that growing cancer cells in 3D culture mimics more closely the *in vivo* environment compared with traditional two dimensional (2D) cell culture systems (25-28). In this sense, 3D-cultured breast cancer cells are able to provide more accurate evidence of the drug's activity in development of novel therapeutics (25). The actual tumor microenvironment in the human body consists of cancer cells, fibroblasts, endothelial cells and extracellular matrix (26). In comparison with 2D cell-culture systems, the specific characteristics of 3D-culture systems include tight cell-cell interactions, cell-microenvironment interactions, and special internal and external cellular structures (27,28).

The aim of the present study was to investigate the effects of As₂S₂ on MCF-7 cells (a human breast cancer cell line), and to further disclose the possible molecular mechanisms underlying the action of the drug. In the present study, 2D- and 3D-cell culture systems were introduced in order to observe and compare the cell formation, cellular architecture, and drug responses between the two culture systems, and to evaluate the effects of As₂S₂ on MCF-7 cells cultured in the two systems.

Materials and methods

Reagents. The cell counting kit-8 (CCK8) was obtained from Dojindo Molecular Technologies, Inc. (Tokyo, Japan). The fluorescein isothiocyanate (FITC) Annexin V Apoptosis Detection kit was from BD Biosciences (San Diego, CA, USA). The ECL™ Western Blotting Analysis system and ECL™ Prime Western Blotting Detection reagent were purchased from GE Healthcare (Buckinghamshire, UK). As₂S₂ and mouse anti-human Bcl-2-associated X protein (Bax) were purchased from Sigma-Aldrich (Merck KGaA, Darmstadt, Germany). The Pro-Survival Bcl-2 Family Antibody Sampler kit, rabbit anti-human phosphoinositol 3-kinase (PI3K), rabbit anti-human Akt, and rabbit anti-human mammalian target of rapamycin (mTOR) were obtained from Cell Signaling Technology, Inc. (Danvers, MA, USA). Mouse anti-human caspase-7 was purchased from BD Pharmingen (BD Biosciences, San Jose, CA, USA). Mouse anti-human p53 was obtained from BioLegend, Inc. (San Diego, CA, USA).

Cell lines and cell culture. The human breast cancer cell line, MCF-7, and the human normal breast cell line, 184B5, were purchased from the American Type Culture Collection (Manassas, VA, USA). MCF-7 cells were cultured in Alpha-MEM medium (Gibco; Thermo Fisher Scientific, Inc., Waltham, MA, USA) supplemented with penicillin, streptomycin and 10% fetal bovine serum (Merck KGaA, Darmstadt, Germany). 184B5 cells were cultured in DMEM/F12 medium supplemented with 5% FBS, 1x Insulin, Transferrin and Selenium (ITS; Lonza Group Ltd., Anaheim, CA, USA), 100 nM hydrocortisone (Merck KGaA), 2 mM sodium pyruvate (Lonza Group, Ltd., Chiba, Japan), 20 ng/ml epidermal growth factor, 0.3 nM *trans*-retinoic acid (both from Merck KGaA), 100 U/ml penicillin and 100 µg/ml streptomycin. Cells were maintained as attached cells at 37°C in 5% carbon dioxide in a humidified atmosphere.

2D cell-culture assay. MCF-7 cells were seeded at a density of 10,000 cells/well in 500 µl cell culture media into 48-well plates (Iwaki Co., Ltd., Tokyo, Japan), and then incubated for 24 h. Vehicle for controls (cell culture media) and different concentrations of As₂S₂ were subsequently added into the corresponding wells to adjust the final drug concentrations of As₂S₂ to 0, 4, 8 and 16 µM. MCF-7 cells were allowed to grow for 72 h in the presence of the drug. This was followed by a cytotoxicity assay and other downstream applications, including apoptosis detection and western blotting.

3D cell-culture assay. 3D spheroids were formed using DSeA 3D micro-plates (International Frontier Technology Laboratory, Inc., Tokyo, Japan) with thermo-reversible gelatin polymer (TGP), as described previously (29). Briefly, TGP powder in each well was dissolved in Alpha-MEM medium (Thermo Fisher Scientific, Inc.) and incubated at 4°C overnight to develop the aqueous solution (the sol phase). MCF-7 cells were subsequently seeded into cold Alpha-MEM medium with TGP on ice at a density of 10,000 cells/well, followed by incubation at 37°C to develop the gel form. Vehicle and the drug were applied in the identical manner as described above for the 2D cell culture. MCF-7 cells were incubated in the gel at 37°C for 72 h to develop spheroids (Fig. 1).

Microscopy. The cellular morphological structures of MCF-7 cells in both 2D- and 3D-cultures were observed on the fourth day following seeding using an IX70® inverted microscope (Olympus Corporation, Tokyo, Japan). A series of bright-field images were recorded and examined with 10x, 20x and 40x objectives (original magnifications: x100, x200 and x400, respectively).

Cytotoxicity assay. Cell cytotoxicity was analyzed using a CCK-8 assay (Dojindo Molecular Technologies, Inc.). A total of 1x10⁴ cells/well MCF-7 cells were seeded into 48-well plates (the cell density was 1x10⁴ cells/500 µl), and As₂S₂ was added at final concentrations of 0, 4, 8 and 16 µM. The plate was subsequently incubated at 37°C in a humidified atmosphere of 95% air and 5% CO₂ for 72 h. Following incubation, 25 µl CCK-8 reagent was added into each well, followed by an additional incubation for 3 h at 37°C in a humidified atmosphere. The optical density (OD) value of each well was measured

using a Corona MT P-32 micro-plate reader (Corona Electric Co., Ltd., Ibaraki, Japan) at 570 nm. The cell viability rate was calculated according to the following equation: Cell viability rate = (OD sample value - OD blank value)/(OD control value - OD blank value) x100%.

Assessment of apoptosis. Apoptotic rates of the MCF-7 cells were analyzed using an Annexin V-FITC Apoptosis Detection kit (BD Biosciences). MCF-7 cells (2×10^5 cells/well) were seeded in 24-well plates (cell density, 2×10^5 cells/ml; volume, 1 ml cell suspension/well), and treated with serial concentrations of As_2S_2 (final concentrations: 0, 4, 8 and 16 μM); this was followed by incubation for an additional 72 h. Subsequently, the staining procedure was performed according to the manufacturer's protocol. A total of 1×10^4 cells was analyzed using a flow cytometer (BD Biosciences). The cells were subsequently assessed for viable (Annexin V/PI), early apoptotic (Annexin V⁺/PI⁻), late apoptotic (Annexin V⁺/PI⁺) and necrotic (Annexin V/PI⁺) cells.

Western blotting. A western blotting protocol was utilized in order to evaluate the protein expression levels of Bcl-2, Bax, p53, caspase-7, PI3K, Akt and mTOR in both monolayers and spheroids. Total protein was extracted from the MCF-7 cells treated with various final concentrations of As_2S_2 (0, 4, 8 and 16 μM) in both 2D and 3D cell-culture systems. Briefly, cell lysates were separated by SDS-PAGE and transferred into a polyvinylidene difluoride (PVDF) transfer membrane (Immobilon-P; Merck Millipore, Darmstadt, Germany). Membranes were blocked with 5% skimmed milk for 1 h. The membranes were washed with Tris-buffered saline/0.1% Tween-20 (TBST), and then incubated overnight at 4°C with 1:500 anti-mouse p53 specific antibody (cat. no. 628201; BioLegend, Inc.), 1:500 anti-mouse Bax-specific antibody (cat. no. B8429; Merck KGaA), 1:1,000 anti-mouse caspase-7-specific antibody (cat. no. 551238; BD Biosciences), 1:1,000 anti-rabbit Bcl-2-specific antibody (cat. no. 9941), 1:1,000 anti-rabbit PI3K p85 subunit-specific antibody (cat. no. 4228), 1:1,000 anti-rabbit Akt-specific antibody (cat. no. 4691), and 1:1,000 anti-rabbit mTOR-specific antibody (cat. no. 2983) (all from Cell Signaling Technology, Inc.). Membranes were also probed with mouse anti-human β -actin (cat. no. ab49900; Abcam, Tokyo, Japan) at 1:1,000 dilution as the internal control. The membranes were incubated overnight with the primary antibodies listed above at 4°C. The following day, the blots were incubated with 1:1,000 anti-mouse (cat. no. 7076) or 1:1,000 anti-rabbit (cat. no. 7074) (both from Cell Signaling Technology, Inc.) specific polyclonal secondary antibodies for 1 h at room temperature. The membranes were washed three times with TBST. Signals were detected with an ECL Western Blot detection kit in a luminescent image analyzer (Fujifilm; LAS-3000; Fujifilm, Tokyo, Japan). The images obtained were subsequently quantitatively analyzed using the ImageJ software program (Rasband, W.S., ImageJ, U.S. National Institutes of Health, Bethesda, MD, USA; <http://rsb.info.nih.gov/ij/>).

Statistical analysis. Data are presented as the mean \pm standard error of the mean. One-way analysis of variance (ANOVA) followed by Tukey's post-hoc test was performed for multiple comparisons, whereas Student's t-test was used for the comparison of two groups. $P < 0.05$ was considered to indicate

a statistically significant difference. Each experiment was repeated independently at least three times.

Results

Human normal breast cells 184B5 are less sensitive to As_2S_2 in comparison to MCF-7 cells. In order to determine the cytotoxic selectivity of As_2S_2 , a normal human breast epithelial cell line (184B5) was used as a normal control (30,31), and the cytotoxic effect of As_2S_2 on both the breast cancer cell line (MCF-7) and 184B5 cells was examined using a CCK-8 assay. As shown in Fig. 2, dose-dependent inhibition was observed in the two cell lines following exposure to different concentrations of As_2S_2 (2-16 μM) for 72 h. In comparison with 184B5 cells, however, the MCF-7 cells exhibited significantly higher sensitivity to As_2S_2 , with increased inhibitory ratios in cell viability (Fig. 2A) and decreased IC_{50} values of As_2S_2 (Fig. 2B). These results suggested that As_2S_2 is less cytotoxic to normal breast epithelial cells than it is to breast cancer cells.

Microscopic imaging of 2D cultured and 3D cultured MCF-7 cells. Following treatment with various concentrations (0, 4, 8 and 16 μM) of As_2S_2 for 72 h, the bright-field images of MCF-7 cells in both 2D and 3D cultures were recorded using an inverted microscope (Olympus Corporation) with original magnifications of x100, x200 and x400 (objectives: 10x, 20x and 40x, respectively). As shown in Fig. 3, MCF-7 cells attached simply to the bottom of the wells in a monolayer manner in the 2D culture plates, whereas they formed multicellular spheroids (MCSs) in the 3D culture plates. The morphological changes of MCF-7 cells cultured as 2D monolayers and 3D spheroids following exposure to 0, 4, 8 and 16 μM As_2S_2 were examined. Exposure to a relatively high concentration (i.e., 8 or 16 μM) of As_2S_2 caused substantial morphological defects in both the 2D and 3D culture systems. Specifically, following treatment with As_2S_2 for 72 h, the MCF-7 monolayers in the 2D plates clearly decreased in a dose-dependent manner, whereas the structural integrity of the MCF-7 spheroids in the 3D plates deteriorated and fragmented, with a destructive configuration (Fig. 3). In contrast, treatment with 4 μM As_2S_2 (a relatively low concentration) led to a modest decrease in 2D-cultured MCF-7 cells, whereas it failed to cause any morphological changes in the 3D spheroids.

Cytotoxic effects of As_2S_2 on 2D- and 3D-cultured MCF-7 cells. CCK-8 assays were performed to assess the viability of cells (in both the 2D- and 3D-cell culture systems) exposed to 0-24 μM of As_2S_2 for 72 h. As shown in Fig. 4A, a significant decrease in cell viability was observed in 2D-cultured MCF-7 cells following treatment with various concentrations of As_2S_2 ; this occurred in a dose-dependent manner. Specifically, in comparison with the control group (0 μM As_2S_2), cell viability was markedly reduced to 77.32 ± 3.92 and $15.24 \pm 1.04\%$ after exposure to 2 and 24 μM As_2S_2 , respectively. In contrast, relatively higher concentrations (≥ 8 μM) of As_2S_2 were observed to have a significant dose-dependent inhibitory effect on 3D-cultured MCF-7 cells. There were significant differences between the 2D- and 3D-cultured systems in cell viability following exposure to As_2S_2 with the final drug concentrations

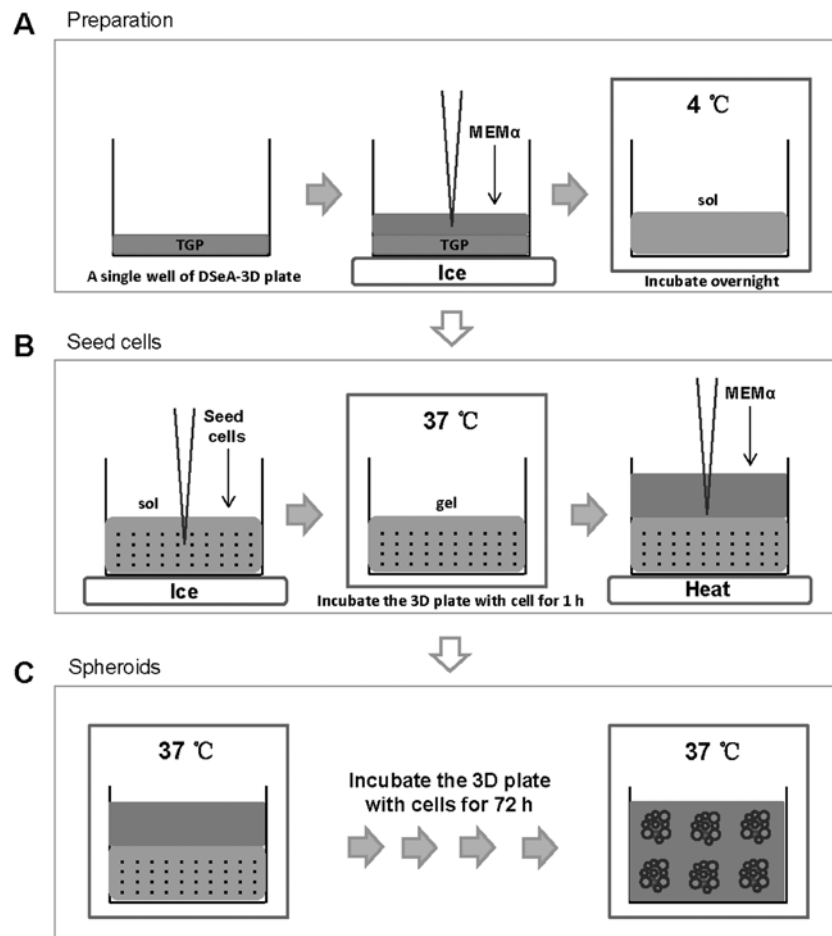


Figure 1. Schematic diagrams of the three-dimensional cell culture system. (A) In a 3D plate, TGP was dissolved in Alpha-MEM (MEM α) medium and incubated at 4°C overnight to develop the aqueous solution (the sol phase). (B) MCF-7 cells were seeded into cold Alpha-MEM medium with TGP (sol phase) on ice, followed by incubation at 37°C for 1 h to develop the gel form. Additional warm Alpha-MEM medium was subsequently added to cover the top of the gel. (C) The MCF-7 cells were incubated in the gel overnight at 37°C for 72 h to develop spheroids. 3D, three-dimensional; TGP, thermo-reversible gelatin polymer.

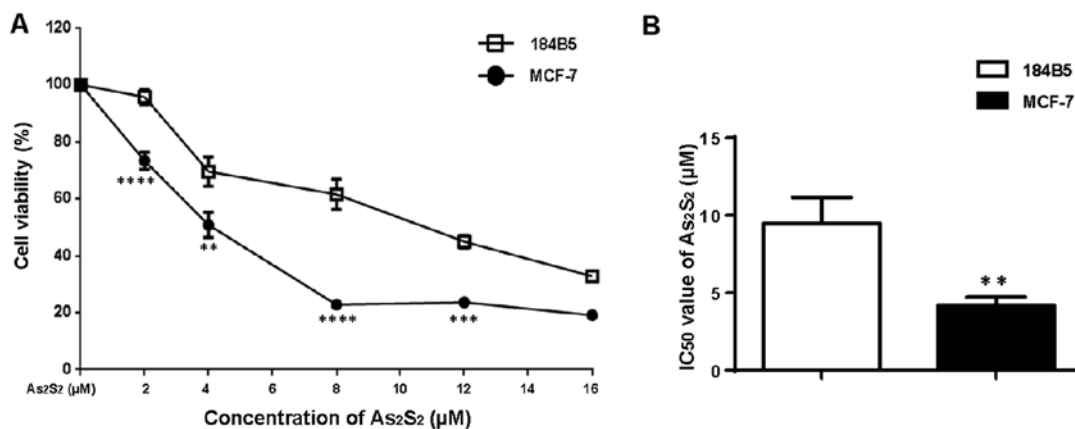


Figure 2. Cytotoxic effects of As₂S₂ on the viability of a human breast cancer cell line, MCF-7, and a human normal breast epithelial cell line, 184B5. (A) Dose-response curves of the viability of MCF-7 and 184B5 cells. (B) The IC₅₀ values of As₂S₂ on MCF-7 and 184B5 cells. Data are expressed as the mean \pm standard error of the mean (n=3). **P<0.01; ***P<0.001; ****P<0.0001 vs. 184B5 cells. As₂S₂, arsenic disulfide.

of 4, 8, 12 and 16 μ M. Although similar dose-dependent growth inhibition was observed in 3D-cultured MCF-7 cells, the growth inhibition rates were much lower compared with those observed in the 2D culture system. In particular, the growth inhibition rates induced by a relatively high concentration ($\geq 8 \mu$ M) of As₂S₂ in the 2D-culture system were more than two

times higher compared with those observed in the 3D culture system, indicating that the MCF-7 spheroids in the 3D culture system were more resistant to the cytotoxicity of As₂S₂ in comparison to the monolayers in the 2D culture system.

The growth inhibition curves were obtained using the probit regression analysis method (Fig. 4B), and the half-maximal

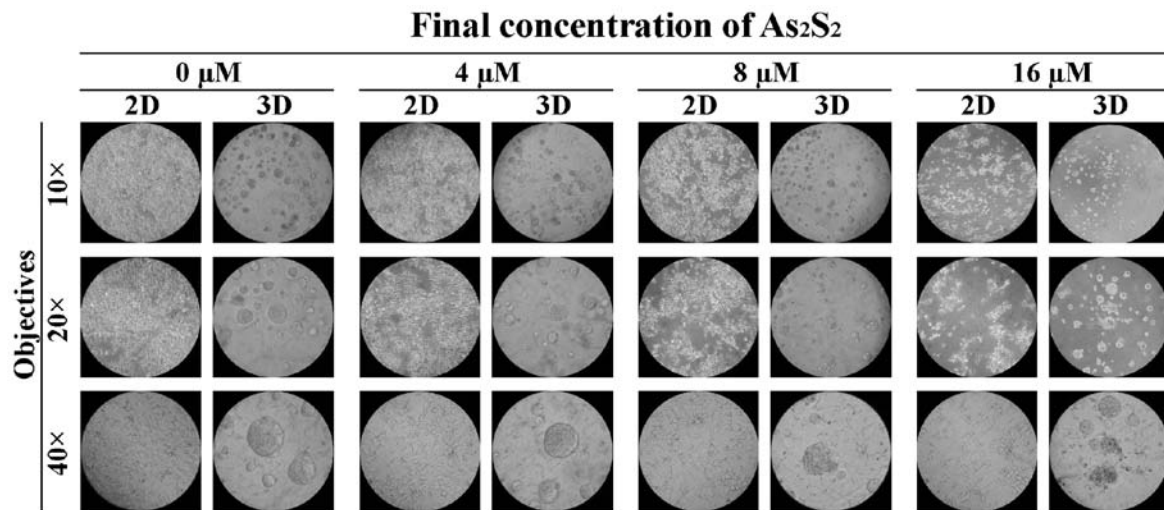


Figure 3. Different morphology of the MCF-7 cells in 2D and 3D cultures and the responses of the monolayers and the spheroids following exposure to As₂S₂. MCF-7 cells were seeded at a density of 10,000 cells/well in the 2D and 3D cultured systems. Subsequently, the cells were treated with a range of concentrations of As₂S₂ (0, 4, 8 and 16 μ M) for 72 h. Bright-field images of MCF-7 monolayers and spheroids were acquired using an IX70[®] inverted microscope (Olympus Corporation, Tokyo, Japan), with x10, x20 and x40 objectives (original magnifications, x100, x200 and x400, respectively). As₂S₂, arsenic disulfide.

inhibitory concentration (IC₅₀ value) of As₂S₂ in the 2D and 3D culture systems was further calculated from their respective inhibition curves. As shown in Fig. 4C, the mean IC₅₀ value of As₂S₂ in the 3D culture system was approximately three times higher compared with that in the 2D culture system (5.11±0.69 μ M in the 2D culture system; 15.65±2.12 μ M in the 3D culture system; P=0.0091). These results suggested that the monolayer cells were more sensitive to As₂S₂ in comparison with the spheroid cells.

As₂S₂ treatment induced apoptosis of 2D- and 3D-cultured MCF-7 cells. To explore whether the induction of apoptosis was involved in the cytotoxicity of As₂S₂ in MCF-7 cells cultured in the 2D and 3D cultured systems, an Annexin V-FITC/PI dual staining assay was performed. The MCF-7 cells of monolayers and spheroids were exposed to 0, 4, 8 and 16 μ M As₂S₂ for 72 h. The number of apoptotic MCF-7 cells was measured by an Annexin V-FITC/PI dual staining assay, followed by flow cytometry, which was based on the probe of the early (Q4) and late apoptosis (Q2) of MCF-7 cells (Fig. 5A).

As shown in Fig. 5B, the early apoptosis of MCF-7 cells was induced by As₂S₂ in a dose-dependent manner in the 2D- and the 3D-culture system. Without any drug exposure, MCF-7 cell spheroids seemed to be more susceptible to early apoptosis than the 2D monolayers, and the median values of the Annexin V⁺/PI⁺ (early apoptosis) cells in the 2D monolayers and the 3D spheroids were 6.65±1.60 and 19.68±1.81%, respectively. The number of early apoptotic cells in the drug-free 3D culture was significantly increased in comparison with the 2D culture (P=0.0017). Following treatment with 4, 8 and 16 μ M of As₂S₂ for 72 h in the 2D culture monolayers, the percentages of cells in early apoptosis were 13.38±3.25% (P=0.5439), 22.40±5.24% (P=0.0340), and 31.08±2.86% (P=0.0017), respectively, in comparison with control (0 μ M As₂S₂). By contrast, following treatment with 4, 8 and 16 μ M of As₂S₂ for 72 h in 3D culture spheroids, the percentages of cells in early apoptosis were 25.63±2.03% (P=0.1628), 30.23±2.29% (P=0.0082), and 34.63±1.10% (P=0.0005), respectively, in comparison with the control.

In the absence of As₂S₂, the 3D spheroids were more susceptible to early apoptosis in comparison with the 2D monolayers. The pro-early apoptotic effects of As₂S₂ between the 2D and 3D systems were therefore compared by evaluating the apoptotic index, i.e., the ratio of apoptotic cell percentages between the drug treatment groups and the control. As shown in Fig. 5C, the early apoptotic indices in the 2D-cultured MCF-7 cells treated with 4, 8 and 16 μ M of As₂S₂ for 72 h increased 2.22±0.50-fold (P=0.8209), 3.95±1.20-fold (P=0.2107), and 5.67±1.51-fold (P=0.0275), respectively, in comparison with the control (1.00). In 3D-cultured spheroids, the early cell-apoptotic indices following treatment with 4, 8 and 16 μ M of As₂S₂ increased 1.33±0.16-fold (P=0.4645), 1.57±0.16-fold (P=0.0988), and 1.82±0.22-fold (P=0.0140), respectively, in comparison with the control (1.00). These data demonstrated that MCF-7 cells cultured as spheroids were more resistant to As₂S₂ in terms of the early induction of apoptosis, in comparison with cells cultured as monolayers, with statistically significant differences in the presence of 8 (P=0.0457) and 16 μ M (P=0.0448) As₂S₂.

As shown in Fig. 5D, late apoptosis of the MCF-7 cells was induced by As₂S₂ in a dose-dependent manner, particularly in 2D monolayers. In 2D culture monolayers, following treatment with 4, 8 and 16 μ M of As₂S₂ for 72 h, the percentages of cells in late apoptosis (Annexin V⁺/PI⁺) were 0.53±0.23% (P=0.9568), 1.17±0.58% (P=0.3166), and 3.60±0.06% (P=0.0005), respectively, in comparison with the control. By contrast, the MCF-7 spheroids were more resistant to As₂S₂-induced late apoptosis, without any significant increases in those cells in the presence of any concentration of As₂S₂.

As shown in Fig. 5E, the late apoptotic index of MCF-7 cells was induced by As₂S₂ in a dose-dependent manner in both 2D- and 3D-culture systems. In 2D culture monolayers, following treatment with 4, 8 and 16 μ M As₂S₂ for 72 h the late cell-apoptotic index increased 2.72±0.49-fold (P=0.8894), 4.48±0.49-fold (P=0.5016), and 8.99±4.52-fold (P=0.0458), respectively, in comparison with the control (1.00). In the 3D-cultured spheroids, following As₂S₂ treatment at

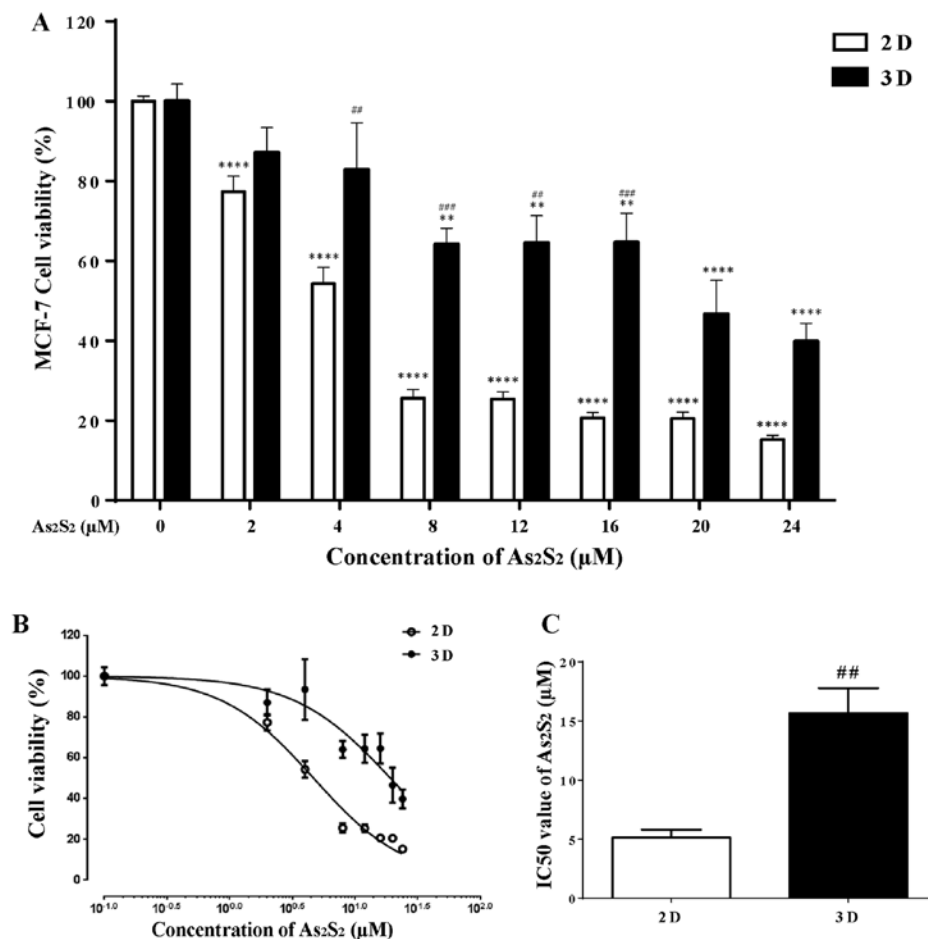


Figure 4. Effects of As₂S₂ on the viability of MCF-7 cells in 2D (open symbol)- and 3D (closed symbol) culture systems. The cells were cultured with serial concentrations of As₂S₂ (0, 2, 4, 8, 12, 16, 20 and 24 μM) for 72 h, and the cell viability was assessed by a WST cell proliferation assay. (A) The cell viability of MCF-7 monolayers and spheroids following exposure to different concentrations of As₂S₂. (B) Dose-response curves for the inhibitory effects of As₂S₂ on the cell viability of 2D-cultured (○) and 3D-cultured (●) MCF-7 cells. (C) The mean IC₅₀ values of As₂S₂ on the MCF-7 cell viabilities in 2D and 3D culture systems. All the data are expressed as the mean ± standard error of the mean (n≥3). Asterisks indicate significant differences between the control and drug treatment groups (**P<0.01; ****P<0.0001). Hashes indicate significant differences between the 2D- and 3D-cultured cells (##P<0.01; ###P<0.001). As₂S₂, arsenic disulfide.

concentrations of 4, 8 and 16 μM for 72 h, the late cell-apoptotic index increased 0.98±0.38-fold (P>0.99), 1.65±0.35-fold (P=0.5419), and 2.63±0.42-fold (P=0.0352), respectively, in comparison with the control (1.00). Therefore, the data in the present study demonstrated that MCF-7 cells cultured as spheroids were more resistant to As₂S₂ in terms of the late induction of apoptosis, in comparison with cells cultured as monolayers, with statistically significant differences in the presence of 4 (P=0.0206) and 8 (P=0.0231) μM As₂S₂, respectively.

Effects of As₂S₂ on the expression of apoptosis-associated proteins in 2D- and 3D- cultured MCF-7 cells. To further investigate the mechanism underlying As₂S₂-induced apoptosis in MCF-7 monolayers and spheroids, the expression levels of apoptosis-associated proteins were evaluated. To accomplish this, the levels of pro-apoptotic proteins, such as Bax, p53 and caspase-7, as well as of the anti-apoptotic protein, Bcl-2, were assessed by western blotting. As shown in Fig. 6A, C and D, the expression levels of the pro-apoptotic proteins, Bax, p53 and caspase-7, were significantly upregulated by As₂S₂ in MCF-7 monolayers. The protein levels of Bax were markedly increased following treatment with 4 (P=0.004), 8 (P=0.0032) and 16 (P=0.0258) μM As₂S₂, in comparison with the control

(0 μM As₂S₂) (Fig. 6A). For p53, the protein levels increased in a dose-dependent manner, following exposure to 4, 8 and 16 μM As₂S₂ (in comparison with the control). A statistically significant increase was observed following treatment with 16 μM As₂S₂ (P=0.0045) (Fig. 6C). The protein expression of caspase-7 was significantly upregulated after incubation with 8 (P=0.0003) and 16 (P=0.0009) μM As₂S₂, in comparison with the control (Fig. 6D). By contrast, a similar increase in the expression level of Bax was confirmed in treated 3D spheroids after treatment with 4, 8 and 16 μM As₂S₂ (P=0.0026, P=0.0265, P=0.0226 vs. control, respectively), and As₂S₂ treatment tended to induce the increased expression of p53; however, the expression of caspase-7 was not significantly increased in the 3D culture system (Fig. 6A, C and D).

As shown in Fig. 6B, following treatment with As₂S₂ for 72 h, the expression of the anti-apoptotic protein, Bcl-2, was down-regulated in both MCF-7 monolayers and spheroids. Following treatment with 16 μM As₂S₂, statistically significant decreases were observed in MCF-7 monolayers (P=0.0221 vs. control) and spheroids (P=0.0051 vs. control) (Fig. 6B).

Effects of As₂S₂ on the expression of pro-survival proteins in 2D- and 3D- cultured MCF-7 cells. Since the PI3K/Akt/mTOR

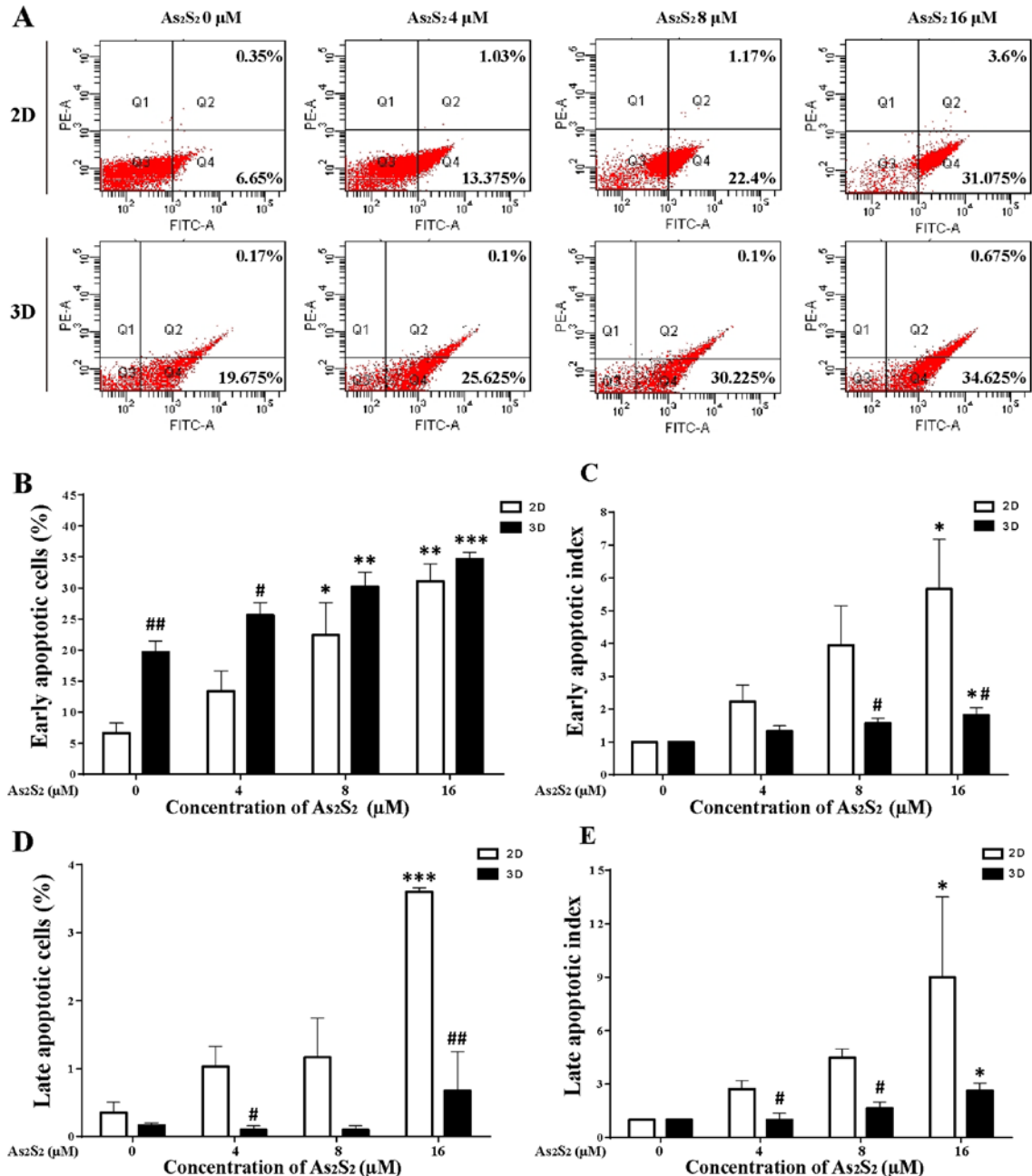


Figure 5. As₂S₂ induces apoptosis in 2D- and 3D-cultured MCF-7 cells. MCF-7 monolayers and spheroids were treated with different concentrations of As₂S₂ (0, 4, 8 and 16 μM) for 72 h. (A) A dot-plot analysis of 2D- and 3D-cultured MCF-7 cells treated with As₂S₂. MCF-7 cells treated with As₂S₂ (0, 4, 8 and 16 μM) were stained with Annexin V/PI and analyzed by flow cytometry. Cells could be classified into four groups based on different quadrants: Viable cells (Q3), early apoptotic cells (Q4), late apoptotic cells (Q2), and necrotic cells (Q1). (B and C) Early apoptosis of MCF-7 cells was induced by As₂S₂ in a dose-dependent manner in the 2D and the 3D culture systems. (D and E) Late apoptosis of MCF-7 cells was induced by As₂S₂ in both the 2D and 3D culture systems. (B and D) show the data for the apoptotic cell percentages, while (C and E) show their indices calculated as relative values in comparison with the control (see the Results section). All data are expressed as the mean ± standard error of the mean (n≥3). Asterisks indicate significant differences between the control and drug treatment groups (*P<0.05; **P<0.01; ***P<0.001). Hashes indicate significant differences between the 2D and 3D culture systems (#P<0.05 and ##P<0.01). As₂S₂, arsenic disulfide.

pathway serves an essential role in cell growth, proliferation, and survival (32,33), the protein expression of these pro-survival mediators were detected in both 2D monolayers and 3D spheroids of MCF-7 cells. Following 72 h of exposure to 4, 8 and 16 μM As₂S₂, the protein levels of PI3K in 2D- and 3D-cultured MCF-7 cells were decreased in a dose-dependent manner in comparison with their untreated counterparts (Fig. 7A). At a concentration of 16 μM, As₂S₂ had a significant inhibitory effect on 2D monolayers (P=0.01). As₂S₂ also induced a significant

downregulation of PI3K in 3D spheroids at final concentrations of 8 (P=0.0066) and 16 (P=0.0001) μM, respectively. As shown in Fig. 7B, subsequently to treatment with As₂S₂ for 72 h, the Akt protein expression levels were downregulated in MCF-7 monolayers and spheroids. After treatment with 16 μM As₂S₂, statistically significant decreases were observed in MCF-7 monolayers (P=0.0031) and spheroids (P=0.0028) (Fig. 7B). Following exposure to 4, 8 and 16 μM As₂S₂, the protein levels of mTOR decreased in a dose-dependent manner in both

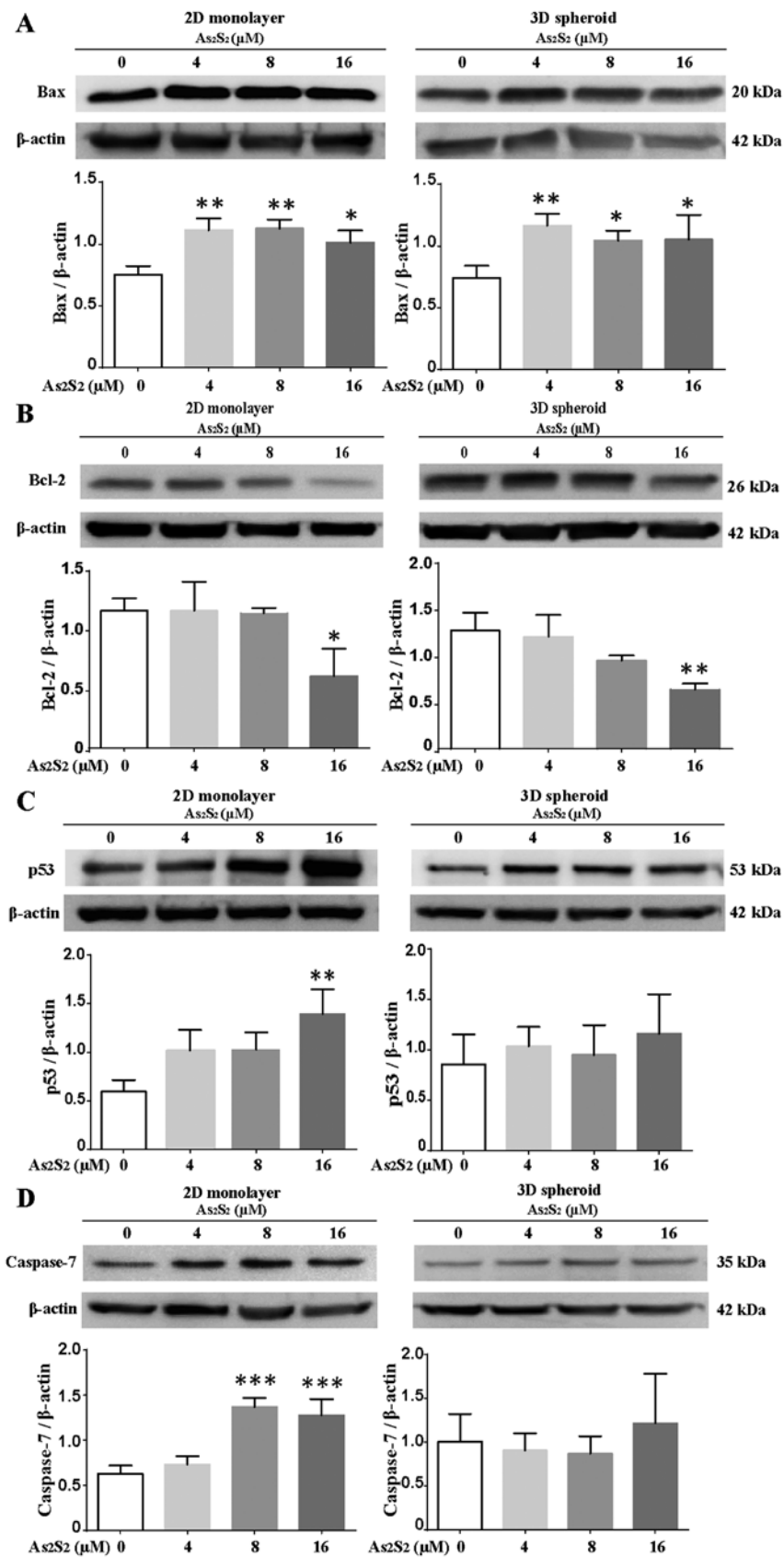


Figure 6. Effects of As₂S₂ on the expression levels of apoptosis-associated proteins in 2D- and 3D-cultured MCF-7 cells. The expression levels of apoptosis-associated proteins were analyzed by western blotting. (A) As₂S₂ significantly increased the levels of the pro-apoptotic protein, Bax, in MCF-7 2D monolayers and 3D spheroids. (B) As₂S₂ significantly reduced the levels of the anti-apoptotic protein, Bcl-2, in MCF-7 2D monolayers and 3D spheroids in a dose-dependent manner. (C) As₂S₂ significantly increased the levels of the pro-apoptotic protein, p53, in MCF-7 2D monolayers in a dose-dependent manner, whereas the agent slightly increased the expression of p53 in MCF-7 3D spheroids. (D) As₂S₂ significantly increased the levels of the pro-apoptotic protein, caspase-7, in MCF-7 2D monolayers in a dose-dependent manner, whereas the agent exerted only a small effect on caspase-7 in MCF-7 3D spheroids. All data are expressed as the mean ± standard error of the mean (n≥3). Asterisks indicate significant differences between the control and drug treatment groups (*P<0.05; **P<0.01; ***P<0.001). As₂S₂, arsenic disulfide; Bcl-2, B-cell lymphoma 2; Bax, Bcl-2-associated X protein.

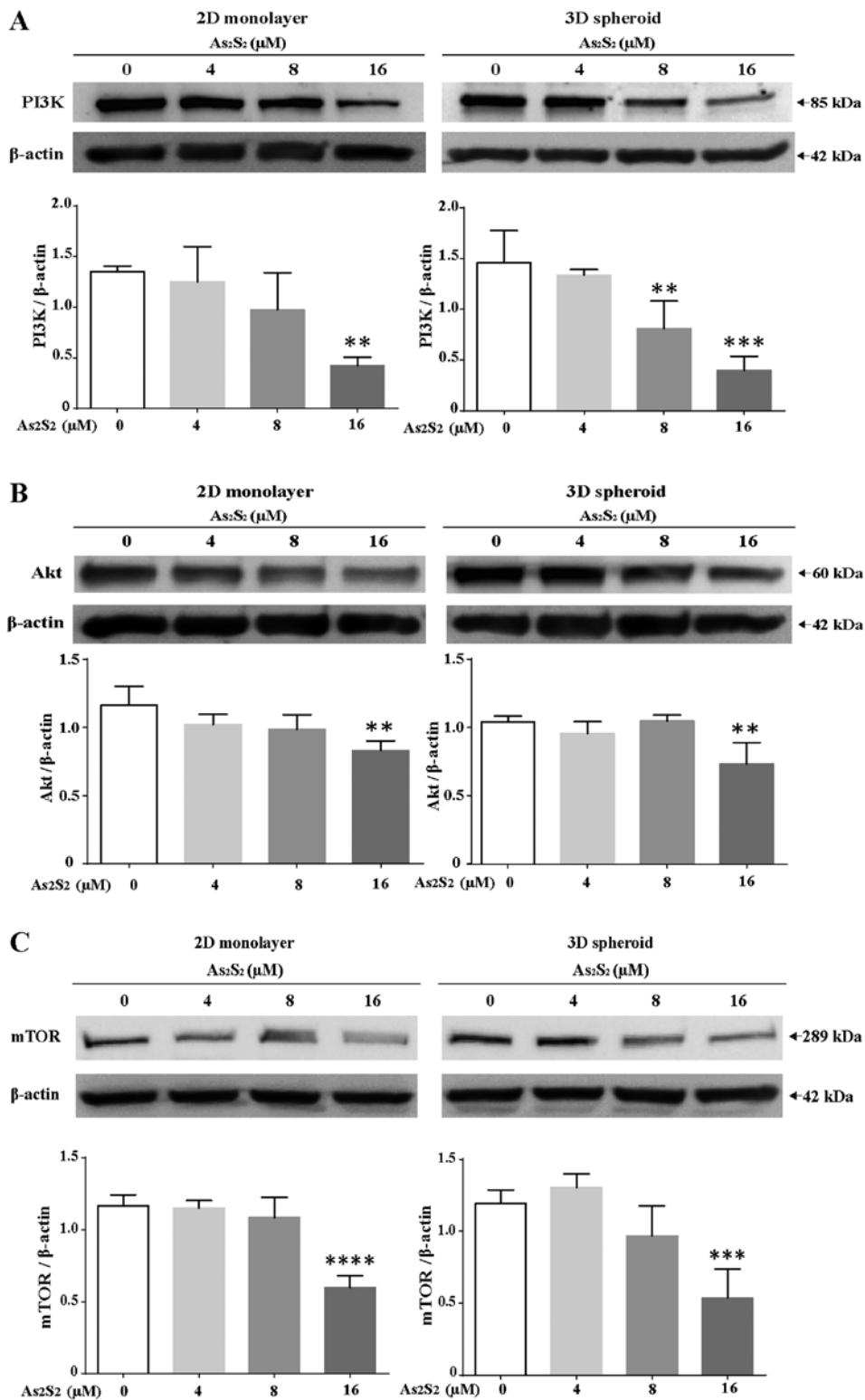


Figure 7. Effects of As₂S₂ on the expression levels of pro-survival proteins in 2D- and 3D-cultured MCF-7 cells. The expression levels of pro-survival proteins were analyzed by western blotting. (A) As₂S₂ significantly reduced the levels of the pro-survival protein, PI3K, in MCF-7 2D monolayers and 3D spheroids in a dose-dependent manner. (B) As₂S₂ significantly reduced the levels of the pro-survival protein, Akt, in MCF-7 2D monolayers and 3D spheroids in a dose-dependent manner. (C) As₂S₂ significantly reduced levels of the pro-survival protein, mTOR, in MCF-7 2D monolayers and 3D spheroids in a dose-dependent manner. All data are expressed as the mean ± standard error of the mean (n≥3). Asterisks indicate significant differences between the control and drug treatment groups (**P<0.01; ***P<0.001; ****P<0.0001). As₂S₂, arsenic disulfide; PI3K, phosphatidylinositol 3-kinase; mTOR, mammalian target of rapamycin.

2D and 3D MCF-7 cells, in comparison with their untreated counterparts; after treatment with 16 μM As₂S₂, statistically significant differences were observed in both 2D monolayers (P<0.0001) and 3D spheroids (P=0.0004) (Fig. 7C).

Discussion

Several arsenic compounds have been investigated for their antitumor potency and efficacy against different breast cancer

cell lines (7-9). For instance, ATO, as a Food and Drug Administration (FDA)-approved drug, was reported to have the potential to suppress cell growth, inhibit cell migration, induce apoptosis and cell cycle arrest, and downregulate cancer pro-coagulant activity in breast cancer cell lines (34-37). However, ATO is regarded as a toxic agent that must be carefully monitored after its intravenous administration. ATO is known to cause severe adverse effects, including liver damage and QT prolongation (10-12). As₂S₂, which shows similar efficacy and fewer adverse effects (14,15), is much less toxic than arsenic trioxide and other common arsenic compounds, including sodium arsenite and arsenate (14,38), and has been considered as an alternative oral arsenic agent for cancer treatment. In China, As₂S₂ has already been approved for clinical use in the treatment of leukemia (16-18,39). A series of clinical studies and trials proved that treatment with As₂S₂ was well tolerated, with only moderate side-effects in patients suffering from APL (13,39,40). Recent studies have also reported the potent anti-tumor properties of As₂S₂ in various solid cancer cell lines, along with a marked reduction in cytotoxic effects in human normal cell lines (41-43). However, there have been very few studies on the anti-tumor effects of As₂S₂ in breast cancer cells (24), and fewer studies on the underlying mechanisms. Therefore, the present study was performed to investigate the anticancer effects of As₂S₂, and the underlying mechanisms in 2D- and 3D-cultured MCF-7 cells. To the best of our knowledge, this is the first report to show the mechanism underlying the cytotoxicity induced by As₂S₂ in MCF-7 cells cultured in 2D and 3D culture systems.

In the present study, an *in vitro* cell culture method was adapted to create 3D spheroids of MCF-7 cells. The 3D cell-culture system established in the present research was based on the adoption of TGP, in which the sol-gel transiting phase is reversibly regulated by temperature (44). By way of comparison, the effects of As₂S₂ on MCF-7 cells cultured as a 2D monolayer were also investigated. The results demonstrated that As₂S₂ decreased the cellular viability of MCF-7 cells by inducing cellular apoptosis in both 2D and 3D cell cultures. These effects were also associated with the activation of pro-apoptotic signals, such as executioner caspase-7, p53 and Bax, and the inhibition of Bcl-2 (associated with anti-apoptotic signaling), as well as the pro-survival PI3K/Akt/mTOR pathway. In addition, the microscopic observations revealed that 2D cells simply attach to the bottom of the wells in a traditional monolayer cell distribution, whereas the 3D cells form multicellular spheroids via cell-cell interactions. The data from the cell viability assays and apoptosis detection experiments revealed that 3D spheroids exhibited a certain degree of drug resistance, in comparison with the 2D monolayer cell culture. This could be attributed to the specific morphological structure of 3D spheroids (Fig. 3), which is similar to the features that studies have previously reported (45,46).

Unregulated cell survival and uncontrolled cell growth may result in excessive cellular proliferation and the loss of controlled cell death, which are two typical phenotypes of cancer cells (47,48), including breast cancer cells. The results obtained from the WST cell proliferation assays demonstrated that As₂S₂ strongly inhibited the cellular viability of MCF-7 cells in a dose-dependent manner, in both 2D monolayers

and in 3D spheroids. Consistently with these findings, the data revealed that As₂S₂ is able to induce apoptosis in 2D- and 3D-cultured MCF-7 cells in a concentration-dependent manner. Since 3D cell-culture models enable cells to form structures that mimic the *in vivo* architecture in a more physiologically relevant condition compared with traditional 2D monolayers (49-51), the present study provided a more reliable method for investigating the actual function of As₂S₂ in MCF-7 cells. In addition, the data of the present study demonstrated the increased drug resistance of MCF-7 cells cultured in a 3D system in comparison with those cultured in a 2D system, either through the inhibition of cell viability or the induction of apoptosis by As₂S₂. Notably, it was revealed that, in the absence of any drug treatment, MCF-7 cell spheroids were more susceptible to apoptosis than the 2D monolayers, which is consistent with observations made by other researchers (52-54). This might be associated with the specific hypoxic and endocrinal changes in the 3D spheroid microenvironment. This phenomenon was different from anoikis (55,56), since the MCF-7 spheroids developed in the present study demonstrated cell-cell interactions and interacted with each other, with the extracellular matrix, and with their microenvironment.

Emerging evidence has demonstrated that arsenic compounds such as arsenic trioxide exert anti-tumor effects by inducing apoptosis in hematological cancer and in solid tumors (6,57,58). The molecular mechanisms underlying arsenic-mediated apoptosis include the activation of intrinsic and extrinsic apoptosis pathways, as well as the suppression of pro-survival pathways in various cancer cell lines. In the current study, the results demonstrated that As₂S₂ induced the expression of pro-apoptotic proteins and inhibited the levels of pro-survival proteins, suggesting the possible pathways responsible for the cytotoxicity of As₂S₂ in MCF-7 cells. Caspases-3 and -7 play critical roles as effectors in the execution phase, namely, the final phase of apoptosis (59,60). Although the expression of caspase-3 was not detected in either 2D monolayers or 3D spheroids (data not shown), the results of the present study indicated that As₂S₂ significantly increased the protein expression of caspase-7 in 2D-cultured MCF-7 cells in a dose-dependent manner. In that respect, the MCF-7 cell apoptosis that was induced by As₂S₂ in the present study might be mediated via the activation of caspase-7 instead of caspase-3, which is congruent with the findings of previous studies showing that the MCF-7 cell line does not express caspase-3, but that it may undergo apoptosis through the activation of caspases-7 and -6 (61,62). The tumor suppressor p53 is capable of inducing cell apoptosis via activation of the mitochondrial and death receptor-induced apoptotic pathways (63,64). The results of the present study revealed that As₂S₂ increased the protein level of p53 in a dose-dependent manner in 2D- and 3D-cultured MCF-7 cells, which is consistent with the results showing that As₂S₂ induced the expression of activated caspase-7 expression in 2D culture. Furthermore, As₂S₂ activated Bax (a pro-apoptotic protein), but inhibited Bcl-2 (an anti-apoptotic protein from the Bcl-2 family), in MCF-7 monolayers as well as in spheroids, indicating the significant role that As₂S₂ exerted in stimulating the intrinsic pathway of apoptosis. The PI3K/Akt/mTOR pathway, which is thought to promote cellular proliferation and survival and

which has been shown to be associated with inactivation of the apoptotic signals, is the most frequently activated signaling pathway in breast cancer (32,33,65,66). Blocking the expression of PI3K/Akt/mTOR simultaneously inhibits cell survival and promotes pro-apoptotic activity. In the present study, the decrease in PI3K/Akt/mTOR expression that occurred in MCF-7 monolayers and spheroids following treatment with As₂S₂ revealed the possible inhibitory role of the arsenic compound in the downregulation of cancer cell-survival signals, which suggests the activation of pro-apoptotic signaling.

In conclusion, the present study has provided evidence that As₂S₂ may be a potential therapeutic agent to be applied in the treatment of breast cancer. The *in vitro* results in the present study suggested that As₂S₂ inhibited the viability of MCF-7 cells and induced cell apoptosis in both 2D monolayers and 3D spheroids in a concentration-dependent manner. Activation of the mitochondrial apoptosis pathway may be involved in this mechanism, since the upregulation of the pro-apoptotic mediators, Bax, p53, caspase-7, as well as the downregulation of the anti-apoptotic mediator, Bcl-2, were observed following exposure to As₂S₂. In addition, the inhibition of the pro-survival PI3K/Akt/mTOR pathway by As₂S₂ treatment contributed to the suppression of cell viability and the induction of apoptosis in 2D- and 3D-cultured MCF-7 cells. Furthermore, the present study has revealed that 3D spheroids of MCF-7 cells had a higher rate of cell viability and reduced cell apoptosis in comparison with 2D monolayer cells following treatment with As₂S₂, indicating the drug resistance of 3D spheroids. However, the present study focused on delineating the pro-apoptotic effect of As₂S₂ in breast cancer cells, and therefore it was confined to one of the cell death mechanisms. Further studies will be performed to elucidate other potential mechanisms involved in the anti-tumor function of As₂S₂, particularly with respect to the induction of cell cycle and autophagy. Furthermore, the mechanism of drug resistance in 3D spheroids also requires further investigation.

Acknowledgements

Not applicable.

Funding

This study was supported in part by grants from China Scholarship Council (file no. 201709110064).

Availability of data and materials

The analyzed data sets generated during the current study are available from the corresponding author on reasonable request for non-commercial purposes, while preserving necessary confidentiality and anonymity.

Authors' contributions

TH conceived the study and was in charge of overall direction and planning and critically revised the manuscript. YXZ designed and performed the experiments, analyzed data and was major contributor in writing the manuscript. KO and BY

gave advice on the experiments and writing of the manuscript and critically revised the manuscript. KO, BY, KS, AK and ST contributed to technical assistance. TH, MS and NT supervised the study. All authors have read and approved the final manuscript.

Ethics approval and consent to participate

Not applicable.

Consent for publication

Not applicable.

Competing interests

The authors declare that they have no competing interests.

References

1. Kamangar F, Dores GM and Anderson WF: Patterns of cancer incidence, mortality, and prevalence across five continents: Defining priorities to reduce cancer disparities in different geographic regions of the world. *J Clin Oncol* 24: 2137-2150, 2006.
2. Parkin DM, Bray F, Ferlay J and Pisani P: Global cancer statistics, 2002. *CA Cancer J Clin* 55: 74-108, 2005.
3. Recht A, Come SE, Henderson IC, Gelman RS, Silver B, Hayes DF, Shulman LN and Harris JR: The sequencing of chemotherapy and radiation therapy after conservative surgery for early-stage breast cancer. *N Engl J Med* 334: 1356-1361, 1996.
4. Rojewski MT, Körper S and Schrezenmeier H: Arsenic trioxide therapy in acute promyelocytic leukemia and beyond: From bench to bedside. *Leuk Lymphoma* 45: 2387-2401, 2004.
5. Cicconi L and Lo-Coco F: Current management of newly diagnosed acute promyelocytic leukemia. *Ann Oncol* 27: 1474-1481, 2016.
6. Miller WH Jr, Schipper HM, Lee JS, Singer J and Waxman S: Mechanisms of action of arsenic trioxide. *Cancer Res* 62: 3893-3903, 2002.
7. Chow SK, Chan JY and Fung KP: Suppression of cell proliferation and regulation of estrogen receptor alpha signaling pathway by arsenic trioxide on human breast cancer MCF-7 cells. *J Endocrinol* 182: 325-337, 2004.
8. Yao M, Yuan B, Wang X, Sato A, Sakuma K, Kaneko K, Komuro H, Okazaki A, Hayashi H, Toyoda H, *et al*: Synergistic cytotoxic effects of arsenite and tetrandrine in human breast cancer cell line MCF-7. *Int J Oncol* 51: 587-598, 2017.
9. Soria EA, Bongiovanni GA, Luján CD and Eynard AR: Effect of arsenite on nitrosative stress in human breast cancer cells and its modulation by flavonoids. *Nutr Cancer* 67: 659-663, 2015.
10. Wu JZ and Ho PC: Comparing the relative oxidative DNA damage caused by various arsenic species by quantifying urinary levels of 8-hydroxy-2'-deoxyguanosine with isotope-dilution liquid chromatography/mass spectrometry. *Pharm Res* 26: 1525-1533, 2009.
11. Horibe Y, Adachi S, Yasuda I, Yamauchi T, Kawaguchi J, Kozawa O, Shimizu M and Moriwaki H: Anticancer effect of arsenite on cell migration, cell cycle and apoptosis in human pancreatic cancer cells. *Oncol Lett* 12: 177-182, 2016.
12. Dangleben NL, Skibola CF and Smith MT: Arsenic immunotoxicity: A review. *Environ Health* 12: 73, 2013.
13. Lu DP, Qiu JY, Jiang B, Wang Q, Liu KY, Liu YR and Chen SS: Tetra-arsenic tetra-sulfide for the treatment of acute promyelocytic leukemia: A pilot report. *Blood* 99: 3136-3143, 2002.
14. Lu YF, Yan JW, Wu Q, Shi JZ, Liu J and Shi JS: Realgar- and cinnabar-containing an-gong-niu-huang wan (AGNH) is much less acutely toxic than sodium arsenite and mercuric chloride. *Chem Biol Interact* 189: 134-140, 2011.
15. Liu J, Liang SX, Lu YF, Miao JW, Wu Q and Shi JS: Realgar and realgar-containing Liu-Shen-Wan are less acutely toxic than arsenite and arsenate. *J Ethnopharmacol* 134: 26-31, 2011.

16. Wang L, Zhou GB, Liu P, Song JH, Liang Y, Yan XJ, Xu F, Wang BS, Mao JH, Shen ZX, *et al.*: Dissection of mechanisms of Chinese medicinal formula Realgar-Indigo naturalis as an effective treatment for promyelocytic leukemia. *Proc Natl Acad Sci USA* 105: 4826-4831, 2008.
17. Zhang QY, Mao JH, Liu P, Huang QH, Lu J, Xie YY, Weng L, Zhang Y, Chen Q, Chen SJ, *et al.*: A systems biology understanding of the synergistic effects of arsenic sulfide and Imatinib in BCR/ABL-associated leukemia. *Proc Natl Acad Sci USA* 106: 3378-3383, 2009.
18. Liu Y, He P, Cheng X and Zhang M: Long-term outcome of 31 cases of refractory acute promyelocytic leukemia treated with compound realgar natural indigo tablets administered alternately with chemotherapy. *Oncol Lett* 10: 1184-1190, 2015.
19. Wu F, Wu D, Ren Y, Duan C, Chen S and Xu A: Bayesian network meta-analysis comparing five contemporary treatment strategies for newly diagnosed acute promyelocytic leukaemia. *Oncotarget* 7: 47319-47331, 2016.
20. Wang L, Liu X, Li X, Lv X, Lu K, Chen N, Li P and Wang X: Arsenic disulfide induces apoptosis of human diffuse large B cell lymphoma cells involving Bax cleavage. *Oncol Rep* 30: 2427-2434, 2013.
21. Cheng YX, Liu R, Wang Q, Li BS, Xu XX, Hu M, Chen L, Fu Q, Pu DM and Hong L: Realgar-induced apoptosis of cervical cancer cell line Siha via cytochrome c release and caspase-3 and caspase-9 activation. *Chin J Integr Med* 18: 359-365, 2012.
22. Song P, Chen P, Wang D, Wu Z, Gao Q, Wang A, Zhu R, Wang Y, Wang X, Zhao L, *et al.*: Realgar transforming solution displays anticancer potential against human hepatocellular carcinoma HepG2 cells by inducing ROS. *Int J Oncol* 50: 660-670, 2017.
23. Wang G, Zhang T, Sun W, Wang H, Yin F, Wang Z, Zuo D, Sun M, Zhou Z, Lin B, *et al.*: Arsenic sulfide induces apoptosis and autophagy through the activation of ROS/JNK and suppression of Akt/mTOR signaling pathways in osteosarcoma. *Free Radic Biol Med* 106: 24-37, 2017.
24. Tian Y, Wang X, Xi R, Pan W, Jiang S, Li Z, Zhao Y, Gao G and Liu D: Enhanced antitumor activity of realgar mediated by milling it to nanosize. *Int J Nanomedicine* 9: 745-757, 2014.
25. Breslin S and O'Driscoll L: Three-dimensional cell culture: The missing link in drug discovery. *Drug Discov Today* 18: 240-249, 2013.
26. Yamada KM and Cukierman E: Modeling tissue morphogenesis and cancer in 3D. *Cell* 130: 601-610, 2007.
27. Weigelt B, Ghajar CM and Bissell MJ: The need for complex 3D culture models to unravel novel pathways and identify accurate biomarkers in breast cancer. *Adv Drug Deliv Rev* 69-70: 42-51, 2014.
28. Rimann M and Graf-Hausner U: Synthetic 3D multicellular systems for drug development. *Curr Opin Biotechnol* 23: 803-809, 2012.
29. Kiyomi A, Makita M, Ozeki T, Li N, Satomura A, Tanaka S, Onda K, Sugiyama K, Iwase T and Hirano T: Characterization and clinical implication of Th1/Th2/Th17 cytokines produced from three-dimensionally cultured tumor tissues resected from breast cancer patients. *Transl Oncol* 8: 318-326, 2015.
30. Dubois V, Jardé T, Delort L, Billard H, Bernard-Gallon D, Berger E, Geloën A, Vasson MP and Caldefie-Chezet F: Leptin induces a proliferative response in breast cancer cells but not in normal breast cells. *Nutr Cancer* 66: 645-655, 2014.
31. Alcolea V, Plano D, Encío I, Palop JA, Sharma AK and Sanmartín C: Chalcogen containing heterocyclic scaffolds: New hybrids with antitumoral activity. *Eur J Med Chem* 123: 407-418, 2016.
32. Ciruelos Gil EM: Targeting the PI3K/AKT/mTOR pathway in estrogen receptor-positive breast cancer. *Cancer Treat Rev* 40: 862-871, 2014.
33. Shaw RJ and Cantley LC: Ras, PI(3)K and mTOR signalling controls tumour cell growth. *Nature* 441: 424-430, 2006.
34. Yun SM, Woo SH, Oh ST, Hong SE, Choe TB, Ye SK, Kim EK, Seong MK, Kim HA, Noh WC, *et al.*: Melatonin enhances arsenic trioxide-induced cell death via sustained upregulation of Redd1 expression in breast cancer cells. *Mol Cell Endocrinol* 422: 64-73, 2016.
35. Zhang S, Ma C, Pang H, Zeng F, Cheng L, Fang B, Ma J, Shi Y, Hong H, Chen J, *et al.*: Arsenic trioxide suppresses cell growth and migration via inhibition of miR-27a in breast cancer cells. *Biochem Biophys Res Commun* 469: 55-61, 2016.
36. Zhang YF, Zhang M, Huang XL, Fu YJ, Jiang YH, Bao LL, Maimaitiyiming Y, Zhang GJ, Wang QQ and Naranmandura H: The combination of arsenic and cryptotanshinone induces apoptosis through induction of endoplasmic reticulum stress-reactive oxygen species in breast cancer cells. *Metallomics* 7: 165-173, 2015.
37. Kasukabe T, Okabe-Kado J, Kato N, Honma Y and Kumakura S: Cotylenin A and arsenic trioxide cooperatively suppress cell proliferation and cell invasion activity in human breast cancer cells. *Int J Oncol* 46: 841-848, 2015.
38. Luo XQ, Ke ZY, Huang LB, Guan XQ, Zhang YC and Zhang XL: Improved outcome for Chinese children with acute promyelocytic leukemia: A comparison of two protocols. *Pediatr Blood Cancer* 53: 325-328, 2009.
39. Zhu HH, Wu DP, Jin J, Li JY, Ma J, Wang JX, Jiang H, Chen SJ and Huang XJ: Oral tetra-arsenic tetra-sulfide formula versus intravenous arsenic trioxide as first-line treatment of acute promyelocytic leukemia: A multicenter randomized controlled trial. *J Clin Oncol* 31: 4215-4221, 2013.
40. Xiang-Xin L, Lu-Qun W, Hao L, Xiao-Peng H, Fang-Lin L, Ling-Ling W, Xue-Liang C and Ming H: Clinical study on prospective efficacy of all-trans Acid, realgar-indigo naturalis formula combined with chemotherapy as maintenance treatment of acute promyelocytic leukemia. *Evid Based Complement Alternat Med* 2014: 987560, 2014.
41. Wu JZ and Ho PC: Evaluation of the in vitro activity and in vivo bioavailability of realgar nanoparticles prepared by cryogrinding. *Eur J Pharm Sci* 29: 35-44, 2006.
42. Wang H, Liu Z, Gou Y, Qin Y, Xu Y, Liu J and Wu JZ: Apoptosis and necrosis induced by novel realgar quantum dots in human endometrial cancer cells via endoplasmic reticulum stress signaling pathway. *Int J Nanomedicine* 10: 5505-5512, 2015.
43. Ding W, Zhang L, Kim S, Tian W, Tong Y, Liu J, Ma Y and Chen S: Arsenic sulfide as a potential anti cancer drug. *Mol Med Rep* 11: 968-974, 2015.
44. Tsukikawa S, Matsuoka H, Kurahashi Y, Konno Y, Satoh K, Satoh R, Isogai A, Kimura K, Watanabe Y, Nakano S, *et al.*: A new method to prepare multicellular spheroids in cancer cell lines using a thermo-reversible gelation polymer. *Artif Organs* 27: 598-604, 2003.
45. Khaitan D, Chandna S, Arya MB and Dwarakanath BS: Establishment and characterization of multicellular spheroids from a human glioma cell line; Implications for tumor therapy. *J Transl Med* 4: 12, 2006.
46. Edmondson R, Broglie JJ, Adcock AF and Yang L: Three-dimensional cell culture systems and their applications in drug discovery and cell-based biosensors. *Assay Drug Dev Technol* 12: 207-218, 2014.
47. Biswas DK, Shi Q, Baily S, Strickland I, Ghosh S, Pardee AB and Iglehart JD: NF-kappa B activation in human breast cancer specimens and its role in cell proliferation and apoptosis. *Proc Natl Acad Sci USA* 101: 10137-10142, 2004.
48. Vermeulen K, Berneman ZN and Van Bockstaele DR: Cell cycle and apoptosis. *Cell Prolif* 36: 165-175, 2003.
49. Fischbach C, Chen R, Matsumoto T, Schmelzle T, Brugge JS, Polverini PJ and Mooney DJ: Engineering tumors with 3D scaffolds. *Nat Methods* 4: 855-860, 2007.
50. Debnath J and Brugge JS: Modelling glandular epithelial cancers in three-dimensional cultures. *Nat Rev Cancer* 5: 675-688, 2005.
51. Breslin S and O'Driscoll L: The relevance of using 3D cell cultures, in addition to 2D monolayer cultures, when evaluating breast cancer drug sensitivity and resistance. *Oncotarget* 7: 45745-45756, 2016.
52. Zeng H, Sun M, Zhou C, Yin F, Wang Z, Hua Y and Cai Z: Hematoporphyrin monomethyl ether-mediated photodynamic therapy selectively kills sarcomas by inducing apoptosis. *PLoS One* 8: e77727, 2013.
53. Akeda K, Nishimura A, Satonaka H, Shintani K, Kusuzaki K, Matsumine A, Kasai Y, Masuda K and Uchida A: Three-dimensional alginate spheroid culture system of murine osteosarcoma. *Oncol Rep* 22: 997-1003, 2009.
54. Chandrasekaran S, Marshall JR, Messing JA, Hsu JW and King MR: TRAIL-mediated apoptosis in breast cancer cells cultured as 3D spheroids. *PLoS One* 9: e11487, 2014.
55. Sodek KL, Murphy KJ, Brown TJ and Ringuette MJ: Cell-cell and cell-matrix dynamics in intraperitoneal cancer metastasis. *Cancer Metastasis Rev* 31: 397-414, 2012.
56. Daubriac J, Fleury-Feith J, Kheuang L, Galipon J, Saint-Albin A, Renier A, Giovannini M, Galateau-Sallé F and Jaurand MC: Malignant pleural mesothelioma cells resist anoikis as quiescent pluricellular aggregates. *Cell Death Differ* 16: 1146-1155, 2009.
57. Khairul I, Wang QQ, Jiang YH, Wang C and Naranmandura H: Metabolism, toxicity and anticancer activities of arsenic compounds. *Oncotarget* 8: 23905-23926, 2017.
58. Boehme KA, Nitsch J, Riester R, Handgretinger R, Schleicher SB, Kluba T and Traub F: Arsenic trioxide potentiates the effectiveness of etoposide in Ewing sarcomas. *Int J Oncol* 49: 2135-2146, 2016.

59. Kadam CY and Abhang SA: Apoptosis markers in breast cancer therapy. *Adv Clin Chem* 74: 143-193, 2016.
60. Earnshaw WC, Martins LM and Kaufmann SH: Mammalian caspases: Structure, activation, substrates, and functions during apoptosis. *Annu Rev Biochem* 68: 383-424, 1999.
61. Kurokawa H, Nishio K, Fukumoto H, Tomonari A, Suzuki T and Saijo N: Alteration of caspase-3 (CPP32/Yama/apopain) in wild-type MCF-7, breast cancer cells. *Oncol Rep* 6: 33-37, 1999.
62. Simstein R, Burow M, Parker A, Weldon C and Beckman B: Apoptosis, chemoresistance, and breast cancer: Insights from the MCF-7 cell model system. *Exp Biol Med (Maywood)* 228: 995-1003, 2003.
63. Wang X, Simpson ER and Brown KA: p53: Protection against tumor growth beyond effects on cell cycle and apoptosis. *Cancer Res* 75: 5001-5007, 2015.
64. Pietsch EC, Sykes SM, McMahon SB and Murphy ME: The p53 family and programmed cell death. *Oncogene* 27: 6507-6521, 2008.
65. Thorpe LM, Yuzugullu H and Zhao JJ: PI3K in cancer: Divergent roles of isoforms, modes of activation and therapeutic targeting. *Nat Rev Cancer* 15: 7-24, 2015.
66. Miller TW, Rexer BN, Garrett JT and Arteaga CL: Mutations in the phosphatidylinositol 3-kinase pathway: Role in tumor progression and therapeutic implications in breast cancer. *Breast Cancer Res* 13: 224, 2011.